Search for the Decay of a B^0 or $\overline{B}^0$ Meson to $\overline{K}^{*0}K^0$ or $K^{*0}\overline{K}^0$

B. Aubert, R. Barate, M. Bona, D. Boutigny, F. Couderc,
Y. Karyotakis, J. P. Lees, V. Poireau, V. Tisserand, and A. Zghiche
Laboratoire de Physique des Particules, F-74941 Annecy-le-Vieux, France

E. Grauges
Universitat de Barcelona, Facultat de Fisica Dept. ECM, E-08028 Barcelona, Spain

A. Palano
Università di Bari, Dipartimento di Fisica and INFN, I-70126 Bari, Italy

J. C. Chen, N. D. Qi, G. Rong, P. Wang, and Y. S. Zhu
Institute of High Energy Physics, Beijing 100039, China

G. Eigen, I. Ofte, and B. Stugu
University of Bergen, Institute of Physics, N-5007 Bergen, Norway

G. S. Abrams, M. Battaglia, D. N. Brown, J. Button-Shafer, R. N. Cahn, E. Charles, M. S. Gill,
Y. Groysman, R. G. Jacobsen, J. A. Kadyk, L. T. Kerth, Yu. G. Kolomensky, G. Kukartsev, G. Lynch,
L. M. Mir, P. J. Oddone, T. J. Orimoto, M. Pripstein, N. A. Roe, M. T. Ronan, and W. A. Wenzel
Lawrence Berkeley National Laboratory and University of California, Berkeley, California 94720, USA

P. del Amo Sanchez, M. Barrett, K. E. Ford, T. J. Harrison, A. J. Hart, C. M. Hawkes, S. E. Morgan, and A. T. Watson
University of Birmingham, Birmingham, B15 2TT, United Kingdom

K. Goetzen, T. Held, H. Koch, B. Lewandowski, M. Pelizaeus, K. Peters, T. Schroeder, and M. Steinke
Ruhr Universität Bochum, Institut für Experimentalphysik 1, D-44780 Bochum, Germany

J. T. Boyd, J. P. Burke, W. N. Cottingham, and D. Walker
University of Bristol, Bristol BS8 1TL, United Kingdom

T. Cuhadar-Donszelmann, B. G. Fulsom, C. Hearty, N. S. Knecht, T. S. Mattison, and J. A. McKenna
University of British Columbia, Vancouver, British Columbia, Canada V6T 1Z1

A. Khan, P. Kyberd, M. Saleem, D. J. Sherwood, and L. Teodorescu
Brunel University, Uxbridge, Middlesex UB8 3PH, United Kingdom

V. E. Blinov, A. D. Bukin, V. P. Druzhinin, V. B. Golubev, A. P. Onuchin,
S. I. Serednyakov, Yu. I. Skovpen, E. P. Solodov, and K. Yu Todyshev
Budker Institute of Nuclear Physics, Novosibirsk 630090, Russia

D. S. Best, M. Bondioli, M. Bruinsma, M. Chao, S. Curry, I. Eschrich, D. Kirkby,
A. J. Lankford, P. Lund, M. Mandelkern, R. K. Mommsen, W. Roethel, and D. P. Stoker
University of California at Irvine, Irvine, California 92697, USA

S. Abachi and C. Buchanan
University of California at Los Angeles, Los Angeles, California 90024, USA

S. D. Foulkes, J. W. Gary, O. Long, B. C. Shen, K. Wang, and L. Zhang
University of California at Riverside, Riverside, California 92521, USA

H. K. Hadavand, E. J. Hill, H. P. Paar, S. Rahatlou, and V. Sharma

University of California at San Diego, La Jolla, California 92093, USA

J. W. Berryhill, C. Campagnari, A. Cunha, B. Dahmes, T. M. Hong, D. Kovalskyi, and J. D. Richman
University of California at Santa Barbara, Santa Barbara, California 93106, USA

T. W. Beck, A. M. Eisner, C. J. Flacco, C. A. Heusch, J. Kroseberg, W. S. Lockman, G. Nesom,
T. Schalk, B. A. Schumm, A. Seiden, P. Spradlin, D. C. Williams, and M. G. Wilson
University of California at Santa Cruz, Institute for Particle Physics, Santa Cruz, California 95064, USA

J. Albert, E. Chen, A. Dvoretskii, D. G. Hitlin, I. Narsky, T. Piatenko, F. C. Porter, A. Ryd, and A. Samuel
California Institute of Technology, Pasadena, California 91125, USA

R. Andreassen, G. Mancinelli, B. T. Meadows, and M. D. Sokoloff
University of Cincinnati, Cincinnati, Ohio 45221, USA

F. Blanc, P. C. Bloom, S. Chen, W. T. Ford, J. F. Hirschauer, A. Kreisel, U. Nauenberg,
A. Olivas, W. O. Ruddick, J. G. Smith, K. A. Ulmer, S. R. Wagner, and J. Zhang
University of Colorado, Boulder, Colorado 80309, USA

A. Chen, E. A. Eckhart, A. Soffer, W. H. Toki, R. J. Wilson, F. Winklmeier, and Q. Zeng
Colorado State University, Fort Collins, Colorado 80523, USA

D. D. Altenburg, E. Feltresi, A. Hauke, H. Jasper, A. Petzold, and B. Spaan
Universität Dortmund, Institut für Physik, D-44221 Dortmund, Germany

T. Brandt, V. Klose, H. M. Lacker, W. F. Mader, R. Nogowski,
J. Schubert, K. R. Schubert, R. Schwierz, J. E. Sundermann, and A. Volk
Technische Universität Dresden, Institut für Kern- und Teilchenphysik, D-01062 Dresden, Germany

D. Bernard, G. R. Bonneaud, P. Grenier,[*] E. Latour, Ch. Thiebaux, and M. Verderi
Ecole Polytechnique, LLR, F-91128 Palaiseau, France

D. J. Bard, P. J. Clark, W. Gradl, F. Muheim, S. Playfer, A. I. Robertson, and Y. Xie
University of Edinburgh, Edinburgh EH9 3JZ, United Kingdom

M. Andreotti, D. Bettoni, C. Bozzi, R. Calabrese, G. Cibinetto,
E. Luppi, M. Negrini, A. Petrella, L. Piemontese, and E. Prencipe
Università di Ferrara, Dipartimento di Fisica and INFN, I-44100 Ferrara, Italy

F. Anulli, R. Baldini-Ferroli, A. Calcaterra, R. de Sangro, G. Finocchiaro,
S. Pacetti, P. Patteri, I. M. Peruzzi,[†] M. Piccolo, M. Rama, and A. Zallo
Laboratori Nazionali di Frascati dell'INFN, I-00044 Frascati, Italy

A. Buzzo, R. Capra, R. Contri, M. Lo Vetere, M. M. Macri, M. R. Monge,
S. Passaggio, C. Patrignani, E. Robutti, A. Santroni, and S. Tosi
Università di Genova, Dipartimento di Fisica and INFN, I-16146 Genova, Italy

G. Brandenburg, K. S. Chaisanguanthum, M. Morii, and J. Wu
Harvard University, Cambridge, Massachusetts 02138, USA

R. S. Dubitzky, J. Marks, S. Schenk, and U. Uwer
Universität Heidelberg, Physikalisches Institut, Philosophenweg 12, D-69120 Heidelberg, Germany

W. Bhimji, D. A. Bowerman, P. D. Dauncey, U. Egede,
R. L. Flack, J .A. Nash, M. B. Nikolich, and W. Panduro Vazquez
Imperial College London, London, SW7 2AZ, United Kingdom

X. Chai, M. J. Charles, U. Mallik, N. T. Meyer, and V. Ziegler
University of Iowa, Iowa City, Iowa 52242, USA

J. Cochran, H. B. Crawley, L. Dong, V. Eyges, W. T. Meyer, S. Prell, E. I. Rosenberg, and A. E. Rubin
Iowa State University, Ames, Iowa 50011-3160, USA

A. V. Gritsan
Johns Hopkins University, Baltimore, Maryland 21218, USA

M. Fritsch and G. Schott
Universität Karlsruhe, Institut für Experimentelle Kernphysik, D-76021 Karlsruhe, Germany

N. Arnaud, M. Davier, G. Grosdidier, A. Höcker, F. Le Diberder, V. Lepeltier, A. M. Lutz, A. Oyanguren,
S. Pruvot, S. Rodier, P. Roudeau, M. H. Schune, A. Stocchi, W. F. Wang, and G. Wormser
Laboratoire de l'Accélérateur Linéaire, IN2P3-CNRS et Université Paris-Sud 11,
Centre Scientifique d'Orsay, B.P. 34, F-91898 ORSAY Cedex, France

C. H. Cheng, D. J. Lange, and D. M. Wright
Lawrence Livermore National Laboratory, Livermore, California 94550, USA

C. A. Chavez, I. J. Forster, J. R. Fry, E. Gabathuler, R. Gamet, K. A. George,
D. E. Hutchcroft, D. J. Payne, K. C. Schofield, and C. Touramanis
University of Liverpool, Liverpool L69 7ZE, United Kingdom

A. J. Bevan, F. Di Lodovico, W. Menges, and R. Sacco
Queen Mary, University of London, E1 4NS, United Kingdom

G. Cowan, H. U. Flaecher, D. A. Hopkins, P. S. Jackson, T. R. McMahon, S. Ricciardi, F. Salvatore, and A. C. Wren
University of London, Royal Holloway and Bedford New College, Egham, Surrey TW20 0EX, United Kingdom

D. N. Brown and C. L. Davis
University of Louisville, Louisville, Kentucky 40292, USA

J. Allison, N. R. Barlow, R. J. Barlow, Y. M. Chia, C. L. Edgar,
G. D. Lafferty, M. T. Naisbit, J. C. Williams, and J. I. Yi
University of Manchester, Manchester M13 9PL, United Kingdom

C. Chen, W. D. Hulsbergen, A. Jawahery, C. K. Lae, D. A. Roberts, and G. Simi
University of Maryland, College Park, Maryland 20742, USA

G. Blaylock, C. Dallapiccola, S. S. Hertzbach, X. Li, T. B. Moore, S. Saremi, H. Staengle, and S. Y. Willocq
University of Massachusetts, Amherst, Massachusetts 01003, USA

R. Cowan, G. Sciolla, S. J. Sekula, M. Spitznagel, F. Taylor, and R. K. Yamamoto
Massachusetts Institute of Technology, Laboratory for Nuclear Science, Cambridge, Massachusetts 02139, USA

H. Kim, P. M. Patel, and S. H. Robertson
McGill University, Montréal, Québec, Canada H3A 2T8

A. Lazzaro, V. Lombardo, and F. Palombo
Università di Milano, Dipartimento di Fisica and INFN, I-20133 Milano, Italy

J. M. Bauer, L. Cremaldi, V. Eschenburg, R. Godang, R. Kroeger, D. A. Sanders, D. J. Summers, and H. W. Zhao
University of Mississippi, University, Mississippi 38677, USA

S. Brunet, D. Côté, P. Taras, and F. B. Viaud
Université de Montréal, Physique des Particules, Montréal, Québec, Canada H3C 3J7

H. Nicholson

Mount Holyoke College, South Hadley, Massachusetts 01075, USA

N. Cavallo,[‡] G. De Nardo, F. Fabozzi,[‡] C. Gatto, L. Lista, D. Monorchio, P. Paolucci, D. Piccolo, and C. Sciacca

Università di Napoli Federico II, Dipartimento di Scienze Fisiche and INFN, I-80126, Napoli, Italy

M. Baak, G. Raven, and H. L. Snoek

NIKHEF, National Institute for Nuclear Physics and High Energy Physics, NL-1009 DB Amsterdam, The Netherlands

C. P. Jessop and J. M. LoSecco

University of Notre Dame, Notre Dame, Indiana 46556, USA

T. Allmendinger, G. Benelli, K. K. Gan, K. Honscheid, D. Hufnagel, P. D. Jackson,
H. Kagan, R. Kass, A. M. Rahimi, R. Ter-Antonyan, and Q. K. Wong

Ohio State University, Columbus, Ohio 43210, USA

N. L. Blount, J. Brau, R. Frey, O. Igonkina, M. Lu, C. T. Potter,
R. Rahmat, N. B. Sinev, D. Strom, J. Strube, and E. Torrence

University of Oregon, Eugene, Oregon 97403, USA

F. Galeazzi, A. Gaz, M. Margoni, M. Morandin, A. Pompili,
M. Posocco, M. Rotondo, F. Simonetto, R. Stroili, and C. Voci

Università di Padova, Dipartimento di Fisica and INFN, I-35131 Padova, Italy

M. Benayoun, J. Chauveau, P. David, L. Del Buono, Ch. de la Vaissière, O. Hamon,
B. L. Hartfiel, M. J. J. John, J. Malclès, J. Ocariz, L. Roos, and G. Therin

Universités Paris VI et VII, Laboratoire de Physique Nucléaire et de Hautes Energies, F-75252 Paris, France

P. K. Behera, L. Gladney, and J. Panetta

University of Pennsylvania, Philadelphia, Pennsylvania 19104, USA

M. Biasini, R. Covarelli, and M. Pioppi

Università di Perugia, Dipartimento di Fisica and INFN, I-06100 Perugia, Italy

C. Angelini, G. Batignani, S. Bettarini, F. Bucci, G. Calderini, M. Carpinelli, R. Cenci, F. Forti,
M. A. Giorgi, A. Lusiani, G. Marchiori, M. A. Mazur, M. Morganti, N. Neri, G. Rizzo, and J. Walsh

Università di Pisa, Dipartimento di Fisica, Scuola Normale Superiore and INFN, I-56127 Pisa, Italy

M. Haire, D. Judd, and D. E. Wagoner

Prairie View A&M University, Prairie View, Texas 77446, USA

J. Biesiada, N. Danielson, P. Elmer, Y. P. Lau, C. Lu, J. Olsen, A. J. S. Smith, and A. V. Telnov

Princeton University, Princeton, New Jersey 08544, USA

F. Bellini, G. Cavoto, A. D'Orazio, D. del Re, E. Di Marco, R. Faccini, F. Ferrarotto, F. Ferroni,
M. Gaspero, L. Li Gioi, M. A. Mazzoni, S. Morganti, G. Piredda, F. Polci, F. Safai Tehrani, and C. Voena

Università di Roma La Sapienza, Dipartimento di Fisica and INFN, I-00185 Roma, Italy

M. Ebert, H. Schröder, and R. Waldi

Universität Rostock, D-18051 Rostock, Germany

T. Adye, N. De Groot, B. Franek, E. O. Olaiya, and F. F. Wilson

Rutherford Appleton Laboratory, Chilton, Didcot, Oxon, OX11 0QX, United Kingdom

S. Emery, A. Gaidot, S. F. Ganzhur, G. Hamel de Monchenault,
W. Kozanecki, M. Legendre, G. Vasseur, Ch. Yèche, and M. Zito

DSM/Dapnia, CEA/Saclay, F-91191 Gif-sur-Yvette, France

X. R. Chen, H. Liu, W. Park, M. V. Purohit, and J. R. Wilson
University of South Carolina, Columbia, South Carolina 29208, USA

M. T. Allen, D. Aston, R. Bartoldus, P. Bechtle, N. Berger, A. M. Boyarski, R. Claus, J. P. Coleman,
M. R. Convery, M. Cristinziani, J. C. Dingfelder, J. Dorfan, G. P. Dubois-Felsmann, D. Dujmic, W. Dunwoodie,
R. C. Field, T. Glanzman, S. J. Gowdy, M. T. Graham, V. Halyo, C. Hast, T. Hryn'ova, W. R. Innes,
M. H. Kelsey, P. Kim, D. W. G. S. Leith, S. Li, S. Luitz, V. Luth, H. L. Lynch, D. B. MacFarlane,
H. Marsiske, R. Messner, D. R. Muller, C. P. O'Grady, V. E. Ozcan, A. Perazzo, M. Perl, T. Pulliam,
B. N. Ratcliff, A. Roodman, A. A. Salnikov, R. H. Schindler, J. Schwiening, A. Snyder, J. Stelzer,
D. Su, M. K. Sullivan, K. Suzuki, S. K. Swain, J. M. Thompson, J. Va'vra, N. van Bakel, M. Weaver,
A. J. R. Weinstein, W. J. Wisniewski, M. Wittgen, D. H. Wright, A. K. Yarritu, K. Yi, and C. C. Young
Stanford Linear Accelerator Center, Stanford, California 94309, USA

P. R. Burchat, A. J. Edwards, S. A. Majewski, B. A. Petersen, C. Roat, and L. Wilden
Stanford University, Stanford, California 94305-4060, USA

S. Ahmed, M. S. Alam, R. Bula, J. A. Ernst, V. Jain, B. Pan, M. A. Saeed, F. R. Wappler, and S. B. Zain
State University of New York, Albany, New York 12222, USA

W. Bugg, M. Krishnamurthy, and S. M. Spanier
University of Tennessee, Knoxville, Tennessee 37996, USA

R. Eckmann, J. L. Ritchie, A. Satpathy, C. J. Schilling, and R. F. Schwitters
University of Texas at Austin, Austin, Texas 78712, USA

J. M. Izen, I. Kitayama, X. C. Lou, and S. Ye
University of Texas at Dallas, Richardson, Texas 75083, USA

F. Bianchi, F. Gallo, and D. Gamba
Università di Torino, Dipartimento di Fisica Sperimentale and INFN, I-10125 Torino, Italy

M. Bomben, L. Bosisio, C. Cartaro, F. Cossutti, G. Della Ricca, S. Dittongo, S. Grancagnolo, L. Lanceri, and L. Vitale
Università di Trieste, Dipartimento di Fisica and INFN, I-34127 Trieste, Italy

V. Azzolini and F. Martinez-Vidal
IFIC, Universitat de Valencia-CSIC, E-46071 Valencia, Spain

Sw. Banerjee, B. Bhuyan, C. M. Brown, D. Fortin, K. Hamano,
R. Kowalewski, I. M. Nugent, J. M. Roney, and R. J. Sobie
University of Victoria, Victoria, British Columbia, Canada V8W 3P6

J. J. Back, P. F. Harrison, T. E. Latham, G. B. Mohanty, and M. Pappagallo
Department of Physics, University of Warwick, Coventry CV4 7AL, United Kingdom

H. R. Band, X. Chen, B. Cheng, S. Dasu, M. Datta, K. T. Flood, J. J. Hollar,
P. E. Kutter, B. Mellado, A. Mihalyi, Y. Pan, M. Pierini, R. Prepost, S. L. Wu, and Z. Yu
University of Wisconsin, Madison, Wisconsin 53706, USA

H. Neal
Yale University, New Haven, Connecticut 06511, USA

We present a search for the decay of a B^0 or $\overline{B}^0$ meson to a $\overline{K}^{*0}K^0$ or $K^{*0}\overline{K}^0$ final state, using a sample of approximately 232 million $B\overline{B}$ events collected with the BABAR detector at the PEP-II asymmetric energy e^+e^- collider at SLAC. The measured branching fraction is $\mathcal{B}(B^0 \to \overline{K}^{*0}K^0) + \mathcal{B}(B^0 \to K^{*0}\overline{K}^0) = (0.2^{+0.9}_{-0.8}{}^{+0.1}_{-0.3}) \times 10^{-6}$. We obtain the following upper limit for the branching fraction at 90% confidence level: $\mathcal{B}(B^0 \to \overline{K}^{*0}K^0) + \mathcal{B}(B^0 \to K^{*0}\overline{K}^0) < 1.9 \times 10^{-6}$. We use our result to constrain the Standard Model prediction for the deviation of the CP asymmetry in $B^0 \to \phi K^0$ from $\sin 2\beta$.

I.   INTRODUCTION

This paper describes a search for the decay of a B^0 or $\overline{B}^0$ meson to a $\overline{K}^{*0}K^0$ or $K^{*0}\overline{K}^0$ final state. Henceforth, we use $B^0 \to \overline{K}^{*0}K^0$ to refer to both B^0 and $\overline{B}^0$ decays and to the $\overline{K}^{*0}K^0$ and $K^{*0}\overline{K}^0$ decay channels. In the Standard Model (SM), $B^0 \to \overline{K}^{*0}K^0$ decays are described by $b \to d s\overline{s}$ diagrams such as those shown in Fig. 1. Figure 1(a) illustrates $b \to d$ "penguin" transitions. A so-called rescattering process, effectively a tree-level $b \to d u\overline{u}$ weak decay followed by the long distance production of a $s\overline{s}$ pair, is shown in Fig. 1(b). Other rescattering diagrams, e.g., with an intermediate c quark loop rather than a u quark loop, are also possible. Note that the rescattering diagrams can be considered to be the long distance components of the corresponding penguin diagrams, in which the quark in the intermediate loop approaches its mass shell.

The SM prediction for the branching fraction of $B^0 \to \overline{K}^{*0}K^0$ is about 0.5×10^{-6} [1]–[3]. Extensions to the SM can yield significantly larger branching fractions, however. For example, models incorporating supersymmetry with R-parity violating interactions predict branching fractions as large as about 8×10^{-6} [3]. The event rates corresponding to this latter prediction are well within present experimental sensitivity. Currently, there are no experimental results for $B^0 \to \overline{K}^{*0}K^0$. Searches for the related non-resonant decay $B^0 \to K^-\pi^+K^0$ are reported in Ref. [4].

At present, little experimental information is available for $b \to d$ transitions. Such processes can provide important tests of the quark-flavor sector of the SM as discussed, for example, in Ref. [5]. Our study can also help to clarify issues concerning potential differences between determinations of $\sin2\beta$ from tree- and penguin-dominated processes, where β is an angle of the Unitarity Triangle. Such differences can provide a signal for physics beyond the SM [6]. In particular, our study is relevant for the interpretation of the time dependent CP asymmetry obtained from $B^0 \to \phi K^0$ decays. (For a review of the Unitarity Triangle and $\sin2\beta$ measurements based on $B^0 \to \phi K^0$ decays, see Sec. 12 of Ref. [7].) In the SM, this decay is dominated by the $b \to s$ penguin diagrams shown in Fig. 2(a). In addition, sub-dominant SM processes with a different weak phase, such as those shown in Figs. 2(b) and (c) involving the CKM matrix element V_{ub}, contribute at a level that is believed to be small [8]. The deviation of the CP asymmetry in $B^0 \to \phi K^0$ de-

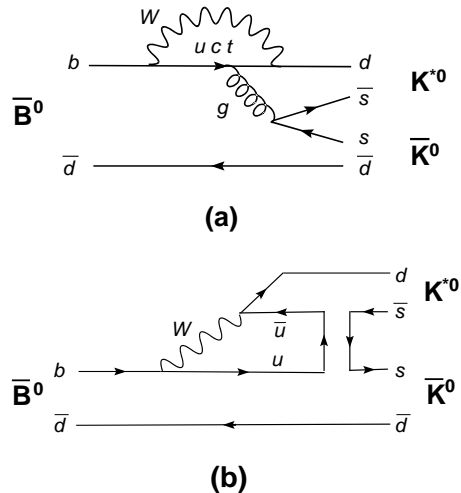*Also at Laboratoire de Physique Corpusculaire, Clermont-Ferrand, France
†Also with Università di Perugia, Dipartimento di Fisica, Perugia, Italy
‡Also with Università della Basilicata, Potenza, Italy

FIG. 1: Feynman diagrams for $\overline{B}^0 \to K^{*0}\overline{K}^0$: (a) penguin diagrams and (b) $b \to u$ rescattering diagram.

cays from $\sin2\beta$ because of these sub-dominant processes is referred to as $\Delta S_{\phi K^0}$.

Grossman *et al.* [9] introduced a method to obtain a SM bound on $\Delta S_{\phi K^0}$, using SU(3) flavor symmetry to relate sub-dominant terms such as those shown in Figs. 2(b) and (c) to the corresponding terms in strangeness-conserving processes such as those shown in Fig. 1. To determine this bound, measurements of the branching fractions of 11 B^0 decay channels are required ($\overline{K}^{*0}K^0$, $K^{*0}\overline{K}^0$, and hh' with $h = \phi$, ω or ρ^0 and $h' = \eta$, η' or π^0). Experimental results are currently available for all these channels except the two in our study: $\overline{K}^{*0}K^0$ and $K^{*0}\overline{K}^0$. Our measurements will therefore enable this bound on $\Delta S_{\phi K^0}$ to be determined for the first time. Note that there are not statistically significant signals for any of the nine channels for which results are currently available.

Our results might also help to constrain predictions for other charmless, strangeness-conserving decays such as $B^0 \to \rho\pi$, in which a $d\overline{d}$ or $u\overline{u}$ pair couples to the gluon in Fig. 1(a) rather than a $s\overline{s}$ pair (see, e.g., Table III of Ref. [2]).

II.   THE BABAR DETECTOR AND DATASET

The data used in this analysis were collected with the BABAR detector at the PEP-II asymmetric e^+e^- storage ring. The data sample consists of an integrated luminosity of 210 fb^{-1} recorded at the $\Upsilon(4S)$ resonance with a center-of-mass (CM) energy of $\sqrt{s} = 10.58$ GeV, corresponding to $(232 \pm 2) \times 10^6$ $B\overline{B}$ events. A data sample of 21.6 fb^{-1} with a CM energy 40 MeV below the $\Upsilon(4S)$ resonance is used to study background con-
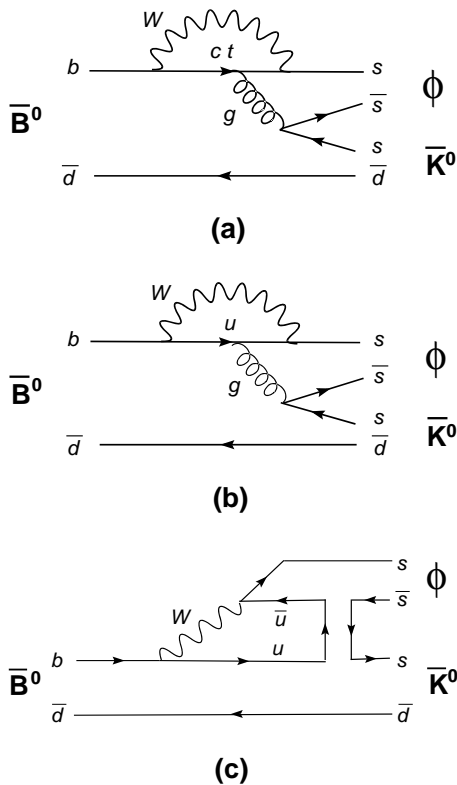
FIG. 2: (a) CKM Dominant and (b,c) CKM suppressed diagrams for $\overline{B}^0 \to \phi\overline{K}^0$.

tributions from light quark $e^+e^- \to q\overline{q}$ ($q = u, d, s$ or c) continuum events.

The *BABAR* detector is described in detail elsewhere [10]. Charged particles are reconstructed using a five-layer silicon vertex tracker (SVT) and a 40-layer drift chamber (DCH) immersed in a 1.5 T magnetic field. Charged pions and kaons are identified (particle identification) with likelihoods for particle hypotheses constructed from specific energy loss measurements in the SVT and DCH and from Cherenkov radiation angles measured in the detector of internally reflected Cherenkov light. Photons are reconstructed in the electromagnetic calorimeter. Muon and neutral hadron identification are performed with the instrumented flux return.

Monte Carlo (MC) events are used to determine signal and background characteristics, optimize selection criteria, and evaluate efficiencies. $B^0\overline{B}^0$ and B^+B^- events, and continuum events, are simulated with the `EvtGen` [11] and `Jetset` [12] event generators, respectively. The effective integrated luminosity of the MC samples is at least four times larger than that of the data for the $B^0\overline{B}^0$ and B^+B^- samples, and about 1.5 times that of the data for the continuum samples. In addition, separate samples of specific $B^0\overline{B}^0$ decay channels are studied for the purposes of background evaluation (see, e.g., the channels mentioned in Sec. III B). All MC samples include simulation of the *BABAR* detector response [13].

III. ANALYSIS METHOD

A. EVENT SELECTION

$B^0 \to \overline{K}^{*0}K^0$ event candidates are selected through identification of $K^{*0} \to K^+\pi^-$ and $K^0 \to K^0_S \to \pi^+\pi^-$ decays. Throughout this paper, the charge conjugate channels are implied unless otherwise noted. As the first step in the selection process, we identify events with at least five charged tracks and less than 20 GeV of total energy. K^0_S candidates are formed by combining all oppositely charged pairs of tracks, by fitting the two tracks to a common vertex, and by requiring the pair to have a fitted invariant mass within 0.025 GeV/c^2 of the nominal K^0_S mass assuming the two particles to be pions. The K^0_S candidate is combined in a vertex fit with two other oppositely charged tracks, associated with the K^{*0} decay, to form a B^0 candidate. These latter two tracks are each required to have a distance of closest approach to the e^+e^- collision point of less than 1.5 cm in the plane perpendicular to the beam axis and 10 cm along the beam axis. Of the two tracks associated with the K^{*0} decay, one is required to be identified as a kaon and the other as a pion using the particle identification. Charged kaons are identified with an efficiency and purity of about 80% and 90%, respectively, averaged over momentum. The corresponding values for charged pions are 90% and 80%.

Our study utilizes an extended maximum likelihood (ML) technique to determine the number of signal and background events (Sec. III C). The fitted experimental variables are ΔE, $m_{\rm ES}$, and the mass of the K^{*0} candidate $M_{K^+\pi^-}$, with $\Delta E \equiv E_B^* - E_{beam}^*$ and $m_{\rm ES} \equiv \sqrt{E_{beam}^{*2} - P_B^{*2}}$ [10], where E_B^* and P_B^* are the CM energy and momentum of the B^0 candidate and E_{beam}^* is half the CM energy. $M_{K^+\pi^-}$ is determined by fitting the tracks from the K^{*0} candidate to a common vertex. We require events entering the ML fit to satisfy the following restrictions:

- $|\Delta E| < 0.15\,{\rm GeV}$,

- $5.2 < m_{\rm ES} < 5.3\,{\rm GeV}/c^2$,

- $0.72 < M_{K^+\pi^-} < 1.20\,{\rm GeV}/c^2$.

Note that virtually all well reconstructed signal events satisfy these criteria.

We further impose the following criteria. The selection values are optimized to minimize the estimated upper limit on the $B^0 \to \overline{K}^{*0}K^0$ branching fraction by comparing the number of expected signal [2] and background events as the selection values are changed.

- B^0 criteria: The χ^2 probability of the fitted B^0 vertex is required to exceed 0.003.

- K^{*0} criteria: K^{*0} candidates are required to satisfy $|\cos\theta_{\rm H}| > 0.50$, where $\theta_{\rm H}$ is the helicity angle in the K^{*0} rest frame, defined as the angle between the direction of the boost from the B^0 rest frame and the K^+ momentum.

- K_S^0 criteria: The χ^2 probability of the fitted K_S^0 vertex is required to exceed 0.06. The fitted K_S^0 mass is required to lie within $10.5\,{\rm MeV}/c^2$ of the peak of the reconstructed K_S^0 mass distribution. (For purposes of comparison, one standard deviation of the K_S^0 mass resolution is about $3\,{\rm MeV}/c^2$.) The K_S^0 decay length significance, defined by the distance between the K^{*0} and K_S^0 decay vertices divided by the uncertainty on that quantity, is required to be larger than 3. The angle between the K_S^0 flight direction and its momentum vector, $\theta_{K_S^0}$, is required to satisfy $\cos\theta_{K_S^0} > 0.997$, where the K_S^0 flight direction is defined by the direction between the K^{*0} and K_S^0 decay vertices.

- Event shape criteria: To separate signal events from the continuum background, we apply selection requirements on global momentum properties. B^0 mesons in $\Upsilon(4S)$ decays are produced almost at rest. Therefore, the B^0 decay products are essentially isotropic in the event CM. In contrast, continuum $e^+e^- \to q\overline{q}$ events at the $\Upsilon(4S)$ energy are characterized by back-to-back two-jet-like event structures because of the relatively small masses of hadrons containing u, d, s and c quarks. As a means to separate signal from continuum background events, we calculate the Legendre polynomial-like terms L_0 and L_2 defined by $L_0 = \sum_{\rm r.o.e.} p_i$ and $L_2 = \sum_{\rm r.o.e.} \frac{p_i}{2}\,(3\cos^2\theta_i - 1)$, where p_i is the magnitude of the 3-momentum of a particle and θ_i is its polar angle with respect to the thrust [14] axis, with the latter determined using the candidate B^0 decay products only. These sums are performed over all particles in the event not associated with the B^0 decay ("rest-of-event" or r.o.e.). L_0 and L_2 are evaluated in the CM frame. We require $0.374\,L_0 - 1.179\,L_2 > 0.15$. The coefficients of L_0 and L_2 are determined with the Fisher discriminant method [15]. To further reduce the continuum background, we also require $|\cos\theta_{\rm T}| < 0.55$, where $\theta_{\rm T}$ is the angle between the momentum of the B^0 candidate and the thrust axis, evaluated in the CM frame, with the thrust axis in this case determined using all particles in the event *except* those associated with the B^0 candidate.

After applying the above criteria, 3.8% of the selected events are found to contain more than one B^0 candidate. For these events, only the candidate with the largest B^0 vertex fit probability is retained.

Our selection procedure eliminates 99.78% and 99.97% of the $B\overline{B}$ and continuum background MC events, respectively, while retaining $9.8 \pm 0.1\%$ of the signal MC events.

B. BACKGROUND EVALUATION

To identify residual backgrounds from B decays, we examine $B^0\overline{B}^0$ and B^+B^- MC events that satisfy the selection criteria of Sec. III A and that fall within the expected signal region of the $m_{\rm ES}$ distribution, defined by $5.271 < m_{\rm ES} < 5.286\,{\rm GeV}/c^2$. The events so-identified are divided into four categories.

1. Events containing B^0 decays with the same $K\pi\pi$ final state as the signal, such as $B^0 \to D^{\mp}K^{\pm}$ ($D^{\mp} \to \pi^{\mp}K_S^0$), $B^0 \to D^{\mp}\pi^{\pm}$ ($D^{\mp} \to K^{\pm}\pi^{\mp}\pi^{\mp}$), or $B^0 \to K^{\pm}\pi^{\mp}K_S^0$. These channels are expected to peak in the signal regions of $m_{\rm ES}$ and ΔE but not in the signal region of $M_{K^+\pi^-}$. The largest number of background events in this category arises from $B^0 \to D^{\mp}K^{\pm}$ ($D^{\mp} \to \pi^{\mp}K_S^0$). To reduce the contributions of this channel, we apply a veto on the $\pi^{\mp}K_S^0$ mass $M_{\pi K_S^0}$ based on the invariant mass of the K_S^0 and the pion used to reconstruct the K^{*0}. A veto with $1.813 < M_{\pi K_S^0} < 1.925\,{\rm GeV}/c^2$ (corresponding to ± 7 standard deviations of a Gaussian fit to the $M_{\pi K_S^0}$ MC distribution) removes $64 \pm 1\%$ of the $D^{\mp}K^{\pm}$ background MC events but only $4.4 \pm 0.6\%$ of the signal MC events, where the uncertainties are statistical. Note that the reconstructed $M_{\pi K_S^0}$ distribution has non-Gaussian tails.

2. Events containing B^0 decays with a kaon misidentified as a pion, such as $B^0 \to \phi K_S^0$ ($\phi \to K^+K^-$) or $B^0 \to f^0 K_S^0$ ($f^0 \to K^+K^-$). This category of background is expected to peak in the $m_{\rm ES}$ signal region, but not in the $M_{K^+\pi^-}$ signal region, and to exhibit a peak in ΔE that is negatively displaced with respect to the signal peak centered at zero. The largest number of events in this category arises from $B^0 \to \phi K_S^0$ ($\phi \to K^+K^-$). We apply a veto on the K^+K^- mass $M_{K^+K^-}$ assuming the pion candidate used to reconstruct the K^{*0} to be a kaon. The veto requires $1.0098 < M_{K^+K^-} < 1.0280\,{\rm GeV}/c^2$ (corresponding to ± 2.5 standard deviations of a Gaussian fit to the $M_{K^+K^-}$ MC distribution). This selection requirement eliminates $87 \pm 1\%$ of the ϕK_S^0 background MC events but only $1.2 \pm 0.3\%$ of the signal MC events.

3. Events containing B^0 decays with a pion misidentified as a kaon, such as $B^0 \to D^{\pm}\pi^{\mp}$ ($D^{\pm} \to \pi^{\pm}K_S^0$) or $B^0 \to \rho^0 K_S^0$ ($\rho^0 \to \pi^{\pm}\pi^{\mp}$). This category of background peaks in the $m_{\rm ES}$ signal region but not in the $M_{K^+\pi^-}$ signal region and exhibits a peak in ΔE that is positively displaced from zero.

4. All remaining $B^0\overline{B}^0$ and B^+B^- MC events that do not fall into the three categories listed above,

such as $B^0 \to K^{*0}\gamma$ $(K^{*0} \to K^{\pm}\pi^{\mp})$, $B^0 \to D^{\mp}K^{\pm}$ $(D^{\mp} \to \mu^-\overline{\nu}_\mu K_s^0)$, or $B^0 \to \eta' K_s^0$ $(\eta' \to \rho^0\gamma)$. These events are characterized both by particle misidentification and an exchange of tracks between the B and $\overline{B}$ decays. This class of events does not peak in ΔE.

Based on scaling to the experimental luminosity, 1.0 event (rounded to the nearest integer) is expected for each of the first three categories, and 54 events for the fourth category.

We also consider potential background from the following source.

5. Events with the same $K\pi\pi$ final state as our signal but with a $K^{\pm}\pi^{\mp}$ S-wave decay amplitude, either non-resonant or produced, e.g., through $B^0 \to K_0^{*0}(1430)K_s^0$ $(K_0^{*0}(1430) \to K^{\pm}\pi^{\mp})$ decays. These channels are expected to peak in the signal regions of m_{ES} and ΔE but not in the signal region of $M_{K^+\pi^-}$.

There are no experimental results for $B^0 \to K_0^{*0}(1430)K_s^0$. Studies [16] of $B^+ \to K^+\pi^+\pi^-$ found a substantial $B^+ \to K_0^{*0}(1430)\pi^+$ resonant component, however. To evaluate this potential source of background, we generate $B^0 \to K_0^{*0}(1430)K_s^0$ $(K_0^{*0}(1430) \to K^+\pi^-)$ MC events. After applying the criteria described in Sec. III A, only $1.4 \pm 0.1\%$ of these events remain. More importantly, the interference between the $K^{*0}(890)$ and S-wave $K\pi$ amplitudes is expected to cancel if the detection efficiency is symmetric in the candidate K^{*0} $\cos\theta_{\mathrm{H}}$ distribution. Through MC study, we verify that our efficiency is symmetric in $\cos\theta_{\mathrm{H}}$ to better than about 10%. This allows us to treat potential S-wave $K^{\pm}\pi^{\mp}$ background as an independent component in the ML fit.

C. FIT PROCEDURE

An unbinned extended maximum likelihood fit is used to determine the number of signal and background events in the data. The extended likelihood function $\mathcal{L}$ is defined by

$$\mathcal{L} = \exp\left(-\sum_{i=1}^{7} n_i\right) \prod_{j=1}^{N}\left[\sum_{i=1}^{7} n_i \mathcal{P}_i\right], \qquad (1)$$

where N is the number of observed events and n_i are the yields of the seven event categories: signal, continuum background, and the five $B\overline{B}$ background categories from Sec. III B. The correlations between the three fitted observables are found to be small ($\lesssim 10\%$ in both signal MC and background). Therefore, we define the functions $\mathcal{P}_i$ to be products of three independent probability density functions (PDFs), one for each of ΔE, m_{ES}, and $M_{K^+\pi^-}$. We account for effects related to residual correlations between the variables through the bias correction

and evaluation of systematic uncertainties discussed in Secs. IV and V.

The signal PDFs are defined by a double Gaussian distribution for ΔE, a Crystal Ball function [17] for m_{ES}, and a Breit-Wigner function for $M_{K^+\pi^-}$. The parameters are fixed to values found from fitting signal MC events. We verify that the signal MC predictions for the ΔE and m_{ES} distributions agree with the measured results from $B^0 \to \phi K_s^0$ decays [18] to within the experimental statistical uncertainties. The ϕK_s^0 channel is chosen for this purpose because of its similarity to the $\overline{K}^{*0}K_s^0$ channel.

Separate PDFs are determined for the continuum background and all five categories of $B\overline{B}$ background itemized in Sec. III B. The background PDFs are defined by combinations of polynomial, Gaussian, ARGUS [19], and Breit-Wigner functions fitted to MC events, with the exception of the PDFs for the S-wave $K^{\pm}\pi^{\mp}$ component for which the ΔE and m_{ES} PDFs are set equal to those of the signal while the $M_{K^+\pi^-}$ PDF is based on the scalar $K\pi$ lineshape determined by the LASS Collaboration [20]. All the fits of PDFs to MC distributions yield values of χ^2 per degree-of-freedom near unity.

The event yields of the continuum and last two categories of $B\overline{B}$ background from Sec. III B are allowed to vary in the fits, while those of the first three categories of $B\overline{B}$ background are set equal to the expected numbers given in Sec. III B. The PDF shape parameters of the continuum events are allowed to vary in the fit, while those of the five $B\overline{B}$ background categories are fixed.

IV. RESULTS

We find 682 data events that satisfy the selection criteria. Application of the ML fit to this sample yields $1.0^{+4.7}_{-3.9}$ signal events and 660 ± 75 continuum events where the uncertainties are statistical. These results and those for the $B\overline{B}$ background yields are given in Table I. Based on the SM branching fraction predictions of Ref. [2], 5 signal events (rounded to the nearest integer) are expected. The number of expected continuum events is 619. The statistical uncertainty of the signal yield is defined by the change in the number of events required to increase the quantity $-2\ln\mathcal{L}$ by one unit from its minimum value, and similarly for the other yields. The statistical significance of the result, defined by the square root of the difference between the value of $-2\ln\mathcal{L}$ for zero signal events and at its minimum, expressed in units of the statistical uncertainty, is 0.28.

Figure 3 shows distributions for each of the fitted variables. To enhance the visibility of a potential signal, events in Fig. 3 are required to satisfy $\mathcal{L}_i(S)/[\mathcal{L}_i(S) + \mathcal{L}_i(B)] > 0.6$, where $\mathcal{L}_i(S)$ is the likelihood function for signal events excluding the PDF of the plotted variable $i = \Delta E$, m_{ES} or $M_{K^+\pi^-}$, and $\mathcal{L}_i(B)$ is the corresponding term for all background components added together. The points with uncertainties show the data. The curves

TABLE I: Results from the maximum likelihood fit. $B\overline{B}$ background categories 4 and 5 refer to the last two categories of background itemized in Sec. III B. The yields for the first three $B\overline{B}$ background categories in Sec. III B are fixed to the estimated values of 1.0 event each. The uncertainties on the yields, fit bias, and efficiencies are statistical.

Parameter	Value
Number of events	682
Signal yield	$1.0^{+4.7}_{-3.9}$
Continuum background yield	660 ± 75
$B\overline{B}$ background category 4 yield	17^{+74}_{-71}
$B\overline{B}$ background category 5 yield	$1.4^{+6.4}_{-5.3}$
ML fit bias (signal bias)	-0.2 ± 0.3
MC signal efficiency (including $D^{\mp}$ and ϕ mass vetos)	$9.8 \pm 0.1\%$
Efficiency corrections	
$\quad K_S^0$ tracking	97.8%
$\quad K^{*0}$ tracking	99.0%
$\quad$ Final-state branching fractions	23.0%
Overall detection efficiency	$2.2 \pm 0.1\%$
$\mathcal{B}(B^0 \to \overline{K}^{*0}K^0)$ $\quad + \mathcal{B}(B^0 \to K^{*0}\overline{K}^0)$	$(0.2^{+0.9}_{-0.8}\,{}^{+0.1}_{-0.3}) \times 10^{-6}$
Significance with systematics (σ)	0.26
90% CL upper limit on $\mathcal{B}(B^0 \to \overline{K}^{*0}K^0) + \mathcal{B}(B^0 \to K^{*0}\overline{K}^0)$	$< 1.9 \times 10^{-6}$

FIG. 3: Distributions of ΔE, m_{ES}, and $M_{K^+\pi^-}$. The points with uncertainties show the data. The curves show projections of the ML fit. A selection requirement on the likelihood ratio has been applied as described in the text. The solid curve shows the sum of all fitted components, including the signal. The dashed curve shows the sum of all background components. The dotted curve (barely visible) shows the signal component.

show projections of the ML fit with the likelihood ratio restriction imposed.

We evaluate potential bias in the fitted signal yield by applying the ML fit to 250 simulated data samples constructed as described below. The number of continuum background events in each sample is derived from a Poisson distribution, with a mean set equal to the number of continuum events found in the data, i.e., 660 events. We generate ΔE, m_{ES}, and $M_{K^+\pi^-}$ continuum distributions for each sample by randomly sampling the continuum PDFs using the appropriate number of events for each sample. The number of $B\overline{B}$ background events in each sample is determined in the analogous manner for each of the five $B\overline{B}$ background categories separately. For the first four categories of $B\overline{B}$ background (all but the scalar $K\pi$ component), the ΔE, m_{ES}, and $M_{K^+\pi^-}$ distributions are generated by randomly selecting the appropriate number of events from the corresponding MC
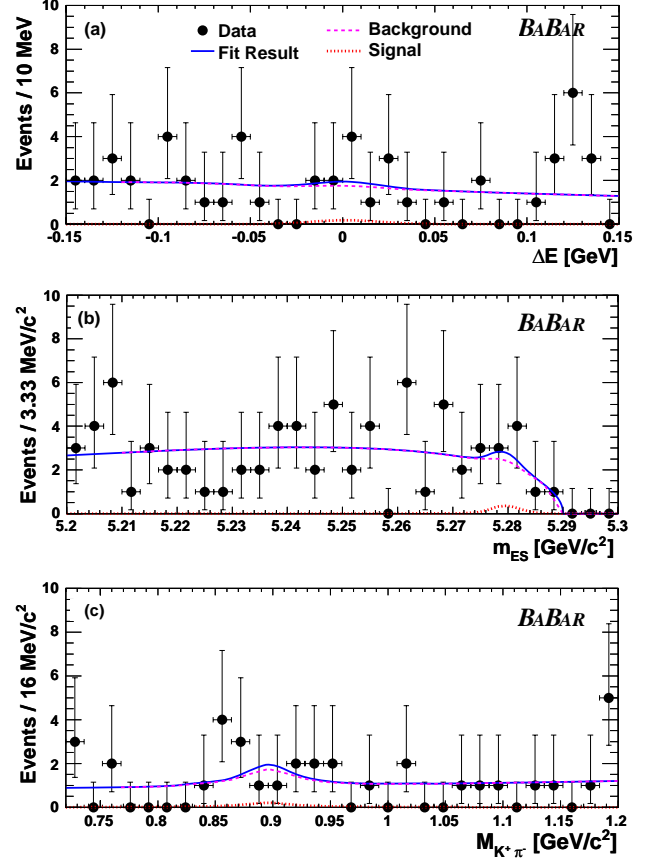
sample. For the scalar $K\pi$ component, the distributions are generated by sampling the PDFs.

The number of signal events in each simulated sample is likewise determined from a Poisson distribution, with a mean N_{sig}^P initially set equal to the fitted signal yield $N_{sig} = 1.0$. The signal ΔE, m_{ES}, and $M_{K^+\pi^-}$ distributions are generated by randomly selecting the appropriate number of signal MC events for each sample. N_{sig}^P is then adjusted until the mean signal yield from the 250 samples equals N_{sig}. The ML fit bias is defined by $N_{bias} = N_{sig} - N_{sig}^P$ and is determined to be -0.2 ± 0.3 (stat.) events. Therefore, the corrected signal yield is $N_{sig} - N_{bias} = 1.2$ events.

In our study, we can distinguish $\overline{K}^{*0}K^0$ from $K^{*0}\overline{K}^0$ events from the sign of the electric charge of the $K^{\pm}$. However, we do not know the flavor of the B meson (B^0 or $\overline{B}^0$) at decay. Therefore, the observed signal yield is related to the sum of the $B^0 \to \overline{K}^{*0}K^0$ and $B^0 \to K^{*0}\overline{K}^0$

branching fractions through

$$\mathcal{B}(B^0 \to \overline{K}^{*0}K^0) + \mathcal{B}(B^0 \to K^{*0}\overline{K}^0) = \frac{N_{sig} - N_{bias}}{\epsilon\, N_{B\overline{B}}},$$
(2)

where ϵ is the overall detection efficiency, given by the product of the MC signal efficiency and three efficiency corrections (Table I). The K_s^0 and K^{*0} tracking corrections account for discrepancies between the data and MC simulation, while the correction for final-state branching fractions accounts for the $K^0 \to K_s^0$, $K_s^0 \to \pi^+\pi^-$, and $K^{*0} \to K^+\pi^-$ branching fractions, which are not incorporated into the simulated signal event sample. The overall efficiency is $\epsilon = 2.2\%$. The factor $N_{B\overline{B}}$ in Eq. (2) is the number of $B\overline{B}$ events in the initial data sample of 210 fb^{-1}. We assume equal decay rates of the $\Upsilon(4S)$ to $B^0\overline{B}^0$ and B^+B^-.

We find the sum of the branching fractions to be $\mathcal{B}(B^0 \to \overline{K}^{*0}K^0) + \mathcal{B}(B^0 \to K^{*0}\overline{K}^0) = (0.2^{+0.9\ +0.1}_{-0.8\ -0.3}) \times 10^{-6}$, where the first uncertainty is statistical and the second is systematic. The systematic uncertainty is discussed in Sec. V. We determine a Bayesian 90% confidence level (CL) upper limit assuming a uniform prior probability distribution. First, the likelihood function is modified to incorporate systematic uncertainties through convolution with a Gaussian distribution whose standard deviation is set equal to the total systematic uncertainty. The 90% CL upper limit is then defined to be the value of the branching fraction below which lies 90% of the total of the integral of the modified likelihood function in the positive branching fraction region. We obtain $\mathcal{B}(B^0 \to \overline{K}^{*0}K^0) + \mathcal{B}(B^0 \to K^{*0}\overline{K}^0) < 1.9 \times 10^{-6}$. We also use the modified likelihood function to determine the significance of our branching fraction result including systematics. This result is listed in Table I.

V. SYSTEMATIC UNCERTAINTIES

To evaluate systematic uncertainties, we consider effects associated with the ML fit, the $B\overline{B}$ background estimates, the efficiency corrections, the total number of $B\overline{B}$ events, and the $K_s^0 \to \pi^+\pi^-$ branching fraction. Table II provides a summary.

To estimate the systematic uncertainty related to the signal PDFs, we independently vary the 11 parameters used to characterize the signal ΔE, $m_{\rm ES}$, and $M_{K^+\pi^-}$ PDFs. The mean and standard deviation of the central ΔE Gaussian distribution, and the mean of the $m_{\rm ES}$ Crystal Ball function, are varied by the statistical uncertainties found by fitting the corresponding quantities to data in a recent study of $B^0 \to \phi K^0$ decays [18]. We vary the standard deviation of the $m_{\rm ES}$ Crystal Ball function to account for observed variations between different run periods. The width of the $M_{K^+\pi^-}$ Breit-Wigner function is varied by ± 0.01 GeV/c^2. The remaining six signal PDF parameters are varied by one standard deviation of their statistical uncertainties found in the fits to the MC dis-

tributions (Sec. III C), taking into account correlations between parameters. For variations of all 11 parameters, the percentage change in the signal yield compared to the standard fit is taken as that parameter's contribution to the overall uncertainty. The total systematic uncertainty associated with the signal PDFs is obtained by adding these 11 contributions in quadrature. The largest contributions are from the variations of the ΔE mean and standard deviation (about 0.3 signal events each).

The systematic uncertainty attributed to the fit bias is defined by adding two terms in quadrature. The first term is the statistical uncertainty of this bias (Table I). The second term is defined by changing the method used to determine the bias. Specifically, we evaluate this bias by generating the ΔE, $m_{\rm ES}$, and $M_{K^+\pi^-}$ distributions of the fourth $B\overline{B}$ background category in Sec. III B using the PDFs rather than sampling MC events, for the 250 simulated data samples: the difference between the results of this method and the standard one allows us to assess the effect of residual correlations between the variables. The fourth category of $B\overline{B}$ background events is chosen because it dominates the $B\overline{B}$ background. The difference between the corrected mean signal yield and the standard result defines the second term.

To estimate an uncertainty associated with the $B\overline{B}$ background, we vary the assumed numbers of events for the three $B\overline{B}$ background categories for which these numbers are fixed, i.e., the first three background categories of Sec. III B. Specifically, we independently vary these numbers by $+2$ and -1 events from their standard values of unity, and determine the quadrature sum of the resulting changes in the signal yield.

A systematic uncertainty associated with the presumed scalar $K\pi$ lineshape is defined by the difference between the signal yield found using the LASS lineshape and a uniform (i.e., flat) $K\pi$ mass distribution.

Systematic uncertainties for the K_s^0 reconstruction efficiency, and for the tracking and particle identification efficiencies of the K^+ and π^- used to reconstruct the K^{*0}, account for known discrepancies between the data and MC simulation for these quantities. Similarly, the MC simulation overestimates the number of selected events compared to data for values of $|\cos\theta_{\rm T}|$ less than about 0.9. We assign a 5% systematic uncertainty to account for this effect.

The systematic uncertainty associated with the number of $B\overline{B}$ pairs is determined to be 1.1%. The uncertainty in the $K_s^0 \to \pi^+\pi^-$ branching fraction is taken from Ref. [7].

The total systematic uncertainty is defined by adding the above-described items in quadrature.

VI. SUMMARY AND DISCUSSION

In this paper, we present the first experimental results for the decay $B^0(\overline{B}^0) \to \overline{K}^{*0}K^0$. From a sample of about 232 million $B\overline{B}$ events, we observe $1.0^{+4.7}_{-3.9}$ $B^0 \to \overline{K}^{*0}K^0$

TABLE II: Summary of systematic uncertainties.

Systematic effect	Uncertainty
ML fit procedure (events)	
Signal PDF parameters	0.5
Fit bias	0.5
$B\overline{B}$ background yields	0.1
Total uncertainty from ML fit (events)	0.7
Scalar $K\pi$ lineshape (events)	$^{+0.0}_{-1.4}$
Efficiency corrections (%)	
K_S^0 reconstruction	1.4%
K^{*0} tracking	2.8%
K^{*0} Particle identification efficiency	0.8%
$\cos\theta_T$ selection requirement	5.0%
Number of $B\overline{B}$ pairs	1.1%
$\mathcal{B}(K_S^0 \to \pi^\pm \pi^\mp)$	0.1%
Total uncertainty from corrections	6.1%
Total systematic uncertainty for $\mathcal{B}(\times 10^6)$	$^{+0.1}_{-0.3}$

event candidates. The corresponding measured sum of branching fractions is $\mathcal{B}(B^0 \to \overline{K}^{*0}K^0) + \mathcal{B}(B^0 \to K^{*0}\overline{K}^0) = (0.2^{+0.9\ +0.1}_{-0.8\ -0.3}) \times 10^{-6}$. We obtain a 90% confidence level upper limit of $\mathcal{B}(B^0 \to \overline{K}^{*0}K^0) + \mathcal{B}(B^0 \to K^{*0}\overline{K}^0) < 1.9 \times 10^{-6}$. This result constrains certain extensions of the SM, such as the R-parity violating supersymmetry models described in Ref. [3].

Our result also can be used to determine an upper bound on $\Delta S_{\phi K^0}$, as mentioned in the introduction. The amplitude A for $B^0 \to \phi K^0$ can be expressed as [9]

$$A = V_{cb}^* V_{cs} a^c + V_{ub}^* V_{us} a^u, \qquad (3)$$

with $a^c = p^c - p^t$ and $a^u = p^u - p^t$, where p^i is the hadronic amplitude of the penguin diagram with intermediate quark $i = u, c$ or t [see Figs. 2(a) and (b)]. The CKM factor multiplying a^u in Eq. (3) is suppressed by $\mathcal{O}(\lambda^2)$ relative to the factor multiplying a^c, where $\lambda = 0.224$ [7] is the sine of the Cabibbo angle. Therefore, the diagrams in Fig. 2(a) are expected to dominate $B^0 \to \phi K^0$ decays. As described in Ref. [9], $\Delta S_{\phi K^0}$ is given by

$$\Delta S_{\phi K^0} = 2\cos 2\beta \, \sin\gamma \, \cos\delta \, \left| \xi_{\phi K^0} \right|, \qquad (4)$$

with

$$\xi_{\phi K^0} \equiv \frac{V_{ub}^* V_{us} \; a^u}{V_{cb}^* V_{cs} \; a^c}, \qquad (5)$$

where δ and γ are the strong and weak phase differences, respectively, between a^u and a^c.

Analogous to Eq. (3), the amplitude A' for $B^0 \to \overline{K}^{*0}K^0$ can be expressed as [9]

$$A' = V_{cb}^* V_{cd}b^c + V_{ub}^* V_{ud}b^u. \qquad (6)$$

In contrast to Eq. (3), neither term in Eq. (6) is suppressed by CKM factors relative to the other. As an effective tree-level process, it is therefore possible that the diagram of Fig. 1(b) dominates $B^0 \to \overline{K}^{*0}K^0$ decays. (This assumption yields the most conservative limit on $\Delta S_{\phi K^0}$.)

The method of Grossman $et\ al.$ [9] consists of using SU(3) flavor symmetry to relate b^c and b^u in Eq. (6) to a^c and a^u in Eq. (3) to obtain a bound on the quantity $\hat{\xi}_{\phi K^0}$ defined by

$$\hat{\xi}_{\phi K^0} \equiv \frac{V_{us}}{V_{ud}} \left(\frac{V_{cb}^* V_{cd}\, a^c + V_{ub}^* V_{ud}\, a^u}{A} \right), \qquad (7)$$

with A given by Eq. (3). The bound on $\hat{\xi}_{\phi K^0}$ is derived using the branching fractions of 11 strangeness-conserving charmless B^0 decays:

$$\left| \hat{\xi}_{\phi K^0} \right| \leq \left| \frac{V_{us}}{V_{ud}} \right| \left\{ 0.5 \sqrt{\frac{2 \left[\mathcal{B}(\overline{K}^{*0}K^0) + \mathcal{B}(K^{*0}\overline{K}^0) \right]}{\mathcal{B}(\phi K^0)}} \right.$$
$$\left. + \sum_{i=1}^{9} C_i \sqrt{\frac{\mathcal{B}(f_i)}{\mathcal{B}(\phi K^0)}} \right\}, \qquad (8)$$

where the C_i are SU(3) coefficients and where the nine final states $f_i = hh'$ are specified in the introduction. $\hat{\xi}_{\phi K^0}$ is related to $\xi_{\phi K^0}$ through [9, 21]

$$|\hat{\xi}_{\phi K^0}|^2 = \frac{\left| \frac{V_{us}V_{cd}}{V_{cs}V_{ud}} \right|^2 + \left| \xi_{\phi K^0} \right|^2 + 2\cos\gamma \, Re\left(\frac{V_{us}V_{cd}}{V_{cs}V_{ud}} \, \xi_{\phi K^0} \right)}{1 + \left| \xi_{\phi K^0} \right|^2 + 2\cos\gamma \, Re\left(\xi_{\phi K^0} \right)}. \qquad (9)$$

The observed rates of strangeness-conserving processes, potentially dominated by $b \to u$ rescattering transitions such as are illustrated in Fig. 1(b), are therefore used to set limits on the contributions of the SM-suppressed $b \to u$ terms shown in Figs. 2(b) and (c), i.e., to set limits on transitions which cause a deviation of the CP asymmetry in $B^0 \to \phi K^0$ decays from $\sin 2\beta$.

We evaluate a 90% CL upper limit on $|\Delta S_{\phi K^0}|$ by generating hypothetical sets of branching fractions for the 11 required SU(3)-related decays: $K^{*0}\overline{K}^0$, $\overline{K}^{*0}K^0$, and hh'. Branching fraction values are chosen using bifurcated Gaussian probability distribution functions with means and bifurcated widths set equal to the measured branching fractions and asymmetric uncertainties. For the measurements of the branching fractions of the nine channels not included in the present study, see Refs. [22, 23]. Negative generated branching fractions are discarded. For each set of hypothetical branching fractions, we compute a bound on $|\Delta S_{\phi K^0}|$ using Eqs. (4) and (8). For

the unknown phase term $\cos\delta$ in Eq. (4), we sample a uniform distribution between -1 and 1. Similarly, the weak phase angle γ is chosen by selecting values from a uniform distribution between 38 and 79 degrees, corresponding to the 95% confidence level interval for γ given in Ref. [24]. (A flat distribution is chosen for γ because the likelihood curve in Ref. [24] is non-Gaussian.) For β, we use $\sin 2\beta = 0.687$ [23]. For each iteration of variables, Eq. (9) is solved numerically for $|\xi_{\phi K^0}|$.

We find that 90% of the hypothetical $|\Delta S_{\phi K^0}|$ bounds lie below 0.42. Our study thus allows the SU(3) bound from Ref. [9], viz., $|\Delta S_{\phi K^0}| < 0.42$ at 90% CL, to be determined for the first time. To assess the contribution of the $\overline{K}^{*0}K^0$ channel on this result, we repeat the procedure described in the previous paragraph with the $B^0 \to \overline{K}^{*0}K^0$ branching fraction and uncertainties set to zero: the corresponding result is 0.32. Potential future measurements of $B^0 \to \overline{K}^{*0}K^0$ yielding a significantly smaller UL and uncertainties would therefore have a significant impact on the $|\Delta S_{\phi K^0}|$ bound. As a cross check, we also determine the SU(3) bound assuming the weak phase angle γ to be distributed according to a Gaussian distribution with a mean of $58.5°$ and a standard deviation of $5.8°$ [25]: this yields $|\Delta S_{\phi K^0}| < 0.43$ at 90% CL. Our analysis does not account for SU(3) flavor breaking effects, generally expected to be on the order of 30%. However, the method is conservative in that it assumes all hadronic amplitudes interfere constructively.

VII. ACKNOWLEDGMENTS

[1] A. Ali, G. Kramer, and C.-D. Lü, Phys. Rev. D **58**, 094009 (1998); Y.-H. Chen, H.-Y. Cheng, B. Tseng, and K.-C. Yang, Phys. Rev. D **60**, 094014 (1999); N.G. Deshpande, B. Dutta, and S. Oh, Phys. Lett. B **473**, 141 (2000); M. Beneke and M. Neubert, Nucl. Phys. B **675**, 333 (2003).

[2] C-W. Chiang, M. Gronau, Z. Luo, J.L. Rosner, and D.A. Suprun, Phys. Rev. D **69**, 034001 (2004).

[3] R. Wang, G.R. Lu, E.-K. Wang, and Y.-D. Yang, hep-ph/0603088.

[4] E. Eckhart *et al.* (CLEO Collaboration), Phys. Rev. Lett. **89**, 251801 (2002); A. Garmash *et al.* (BELLE Collaboration), Phys. Rev. D **69**, 012001 (2004).

[5] R. Fleischer and S. Recksiegel, Phys. Rev. D **71**, 051501(R) (2005).

[6] Y. Grossman and M.P. Worah, Phys. Lett. B **395**, 241 (1997); D. London and A. Soni, Phys. Lett. B **407**, 61 (1997).

[7] S. Eidelman *et al.* (Particle Data Group), Phys. Lett. B **592**, 1 (2004).

[8] Y. Grossman, G. Isidori, and M.P. Worah, Phys. Rev. D **58**, 057504 (1998); M. Beneke, Phys. Lett. B **620**, 143 (2005).

[9] Y. Grossman, Z. Ligeti, Y. Nir, and H. Quinn, Phys. Rev. D **68**, 015004 (2003).

[10] B. Aubert *et al.* (*BABAR* Collaboration), Nucl. Instrum. Meth. A **479**, 1 (2002).

[11] D. Lange, Nucl. Instrum. Meth. A **462**, 152 (2001).

[12] T. Sjöstrand, Comp. Phys. Comm. **82**, 74 (1994).

[13] The *BABAR* detector simulation is based on GEANT4; see Nucl. Instrum. Meth. A **506**, 250 (2003).

[14] S. Brandt *et al.*, Phys. Lett. **12**, 57 (1964); E. Farhi, Phys. Rev. Lett. **39**, 1587 (1977).

[15] R.A. Fisher, Annals of Eugenics, **7** Part II, 179 (1936); see also G. Cowan, *Statistical Data Analysis* (Oxford University Press, New York, 1998).

[16] A. Garmash *et al.* (BELLE Collaboration), Phys. Rev. D **71**, 092003 (2005); B. Aubert *et al.*, (*BABAR* Collaboration), Phys. Rev. D **72**, 072003 (2005).

[17] T. Skwarnicki *et al.* (Crystal Ball Collaboration), DESY Report DESY-F31-86-02, 1986 (unpublished).

[18] B. Aubert *et al.* (*BABAR* Collaboration), Phys. Rev. D **71**, 091102 (2005).

[19] H. Albrecht *et al.* (ARGUS Collaboration), Z. Phys. C

48, 543 (1990).

[20] D. Aston *et al.* (LASS Collaboration), Nucl. Phys. B **296**, 493 (1988).

[21] G. Engelhard, Y. Nir, and G. Raz, Phys. Rev. D **72**, 075013 (2005).

[22] B. Aubert *et al.* (*BABAR* Collaboration), Phys. Rev. Lett. **93**, 181806 (2004); **95**, 131803 (2005); Phys. Rev. D **70**, 032006 (2004).

[23] E. Barberio *et al.* (Heavy Flavor Averaging Group), hep-ex/0603003. (The results for the $B^0 \to \rho^0 \pi^0$ branching fraction are taken from Table 36.)

[24] J. Charles *et al.* (CKMfitter Group), Eur. Phys. J. C **41**, 1 (2005).

[25] M. Bona *et al.* (UTfit Collaboration), JHEP **0507**, 028 (2005).